EUROPEAN ORGANIZATION FOR NUCLEAR RESEARCH

CERN-EP/79-141
15 October 1979

THE PHOTO-IONIZATION PROPORTIONAL SCINTILLATION CHAMBER

G. Charpak*), A. Policarpo**) and F. Sauli
CERN, Geneva, Switzerland

Presented at the
IEEE 1979 Nuclear Science Symposium
San Francisco, 17-19 October 1979

*) Also at the Laboratoire de l'Accélérateur linéaire, Orsay, France.

**) On leave of absence from the Dept. of Physics, Coimbra University, Portugal.

THE PHOTO-IONIZATION PROPORTIONAL SCINTILLATION CHAMBER

G. Charpak*), A. Policarpo**) and F. Sauli
CERN, Geneva, Switzerland

1. Summary

A krypton-filled gas scintillation proportional counter has been coupled, through an ultraviolet transparent LiF window, to a multi-anode proportional chamber operated in a gas mixture (argon-triethylamine-methane) having a large quantum efficiency for the emitted photons. The first experimental results suggest that, in the detection of soft X-rays, one can obtain the good energy resolution characteristics of gas scintillation counters, together with the bi-dimensional coordinate localization typical of multiwire proportional chambers (MWPCs). The name Photo-Ionization Proportional Scintillation chamber (PIPS) is proposed for the device.

2. Coupling the Gas Scintillation Counter to Photo-Ionization Detectors

Gas scintillation proportional counters allow very good energy resolutions to be obtained, close to the statistical limit, over large areas; for a survey of this matter see, for example, the review work of Ref. 1. Since the largest fraction of the secondary light emission induced by electrons in noble gases is peaked in the far or vacuum ultraviolet, several combinations of wavelength shifters and matching phototubes have been used for the detection. Large-area detectors of this kind have been designed for use in astrophysics and in other research fields[2-7]. Bi-dimensional localization can be achieved by mounting several independent photomultipliers to detect the pulse, and performing a weighted average on the signals[5-7]; such systems are, however, intrinsically limited to a single hit per event. Alternative read-out methods using vacuum photodiodes[8] or fibre-optics light-guides to television tubes[9] have been tried, which may overcome the single-hit limitation.

It has recently been proposed to couple a scintillation proportional counter directly to a photo-ionization gaseous detector[10]; indeed, simple calculations show that, if an efficient transfer of photons can be obtained between the two elements, the good energy resolution of the gas scintillation counter could be maintained, taking full advantage of the electronic localization techniques developed for MWPCs. Photo-ionization processes in gases have recently been extensively investigated in connection with Čerenkov ring-imaging devices[11,12]; several combinations of entrance window and photo-ionizing gas have been tried which allow a good quantum efficiency between 11.5 eV (LiF cut-off) and 7.5 eV, the ionization potential of triethylamine, $(C_2H_5)_3N$ or TEA (see Fig. 1)[12]. From a comparison with the known secondary emission spectra for some noble gases (Fig. 2)[13], it can be seen that a suitable combination for the detection of the argon emission is, for example, LiF-benzene, and that for krypton a great variety of windows is available, TEA being a suitable detection medium for the photon. The question of detecting the xenon emission still remains open, since a product having a low enough photo-ionization threshold and a sufficiently high vapour pressure has not yet been found.

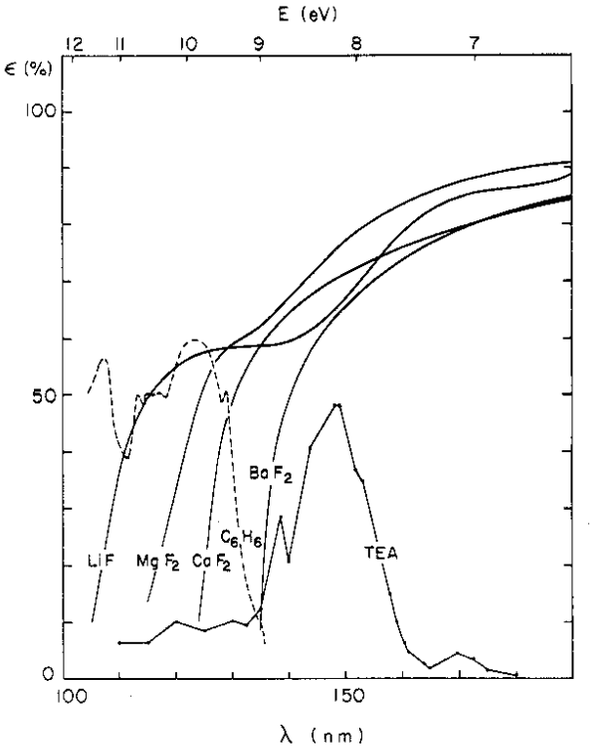

Fig. 1 Compilation of quantum efficiencies of benzene and TEA and of the transparency of several fluoride windows for 5 mm thick crystals as a function of photon wavelength (Ref. 12). Recent evidence suggests that the TEA quantum efficiency shown may be overestimated by a factor of two.

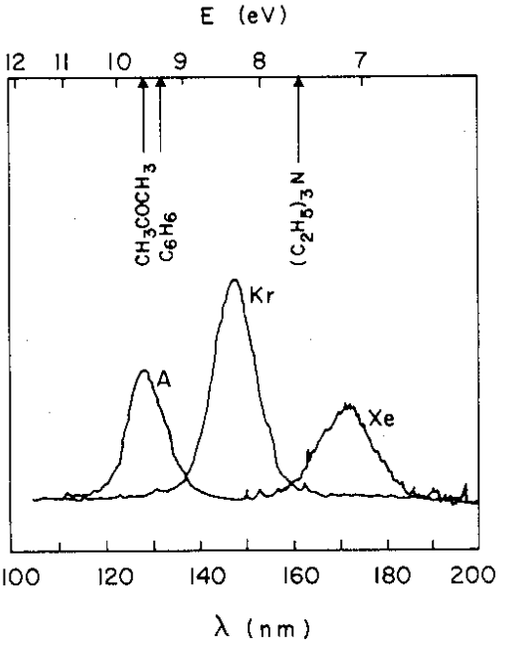

Fig. 2 Spectral distribution of the secondary light emission of pure noble gases, in moderate electric fields, together with the ionization potentials of some vapours (Ref. 13).

*) Also at the Laboratoire de l'Accélérateur linéaire, Orsay, France.

**) On leave of absence from the Dept. of Physics, Coimbra University, Portugal.

3. Description of the detector

To investigate the possibility of coupling the gas scintillation proportional counter to a photo-ionization detector, the structure shown in Fig. 3 was made, using fibre-glass frames. The thicknesses of the so-called absorption and scintillation regions are 10 and 8 mm, respectively. The LiF window is 5 cm in diameter, with a thickness of 5 mm. Its measured transparency is 47.5% at 15° incidence at a wavelength of 150 nm, which is approximately the peak of the emission from krypton (see Fig. 2) and the peak for the photo-ionization of TEA (see Fig. 1). Grids 3 and 4 lie against the LiF window. The distance between the anodes of the multi-anode proportional counter is 2 cm, the anode plane being at 1 cm from grid 4.

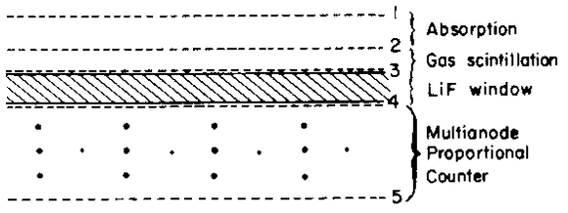

Fig. 3 The photo-ionization proportional scintillation detector (PIPS). Dashed lines represent crossed wire meshes, having wires 50 μm in diameter and 450 μm apart. Grid 4 is laminated. Larger dots represent cathode wires (Ø = 100 μm) and the smaller dots anode wires (Ø = 50 μm).

Energy resolution measurements as well as data on the transfer efficiency were obtained using this detector. For the preliminary data on localization properties, a MWPC was substituted for the multi-anode proportional counter; the anode wires of the MWPC were 2.54 mm apart (Ø = 12 μm), the anode plane being at 5 mm from grid 4.

Both chambers were operated with gases in a flow regime, with krypton on the gas scintillation proportional counter, and a mixture of argon, TEA, and methane on the photo-ionization detector. Although a detailed study of the mixture used on the photo-ionization detector was not made, a few mixtures were tried, e.g. argon with TEA, and also a mixture of these two components with methane. The detection efficiency for photons increases when the concentration of TEA in argon increases up to about 3%, levelling off for higher concentrations. No clear effect on this detection efficiency was seen when methane was added to the mixture of argon and TEA, a slightly better energy resolution being obtained with this last additive with the photo-ionization detector working in the proportional counter region. For all data reported, the mixture used was 83% argon, 3% TEA, and 14% methane.

4. Transfer efficiency

An important parameter that essentially dominates the behaviour of the PIPS detector from the point of view of the energy resolution is $\bar{L}$ (see Ref. 10), i.e. the mean number of detected photoelectrons in the photo-ionization detector per electron produced on the scintillation chamber. As the mean energy required for making an ion pair in the mixture used on the photo-ionization detector is not known, $\bar{L}$ can only be estimated. A convenient approximate assumption is that the mean energy for making an ion pair is the same in this mixture as it is in the filling (krypton) of the gas proportional scintillation counter. Under this assumption, $\bar{L}$ is equal to the transfer efficiency t, i.e. the ratio between the charge collected on the photo-ionization chamber and the charge collected on the same chamber when directly irradiated with the same radiation (see Fig. 3). This PIPS detector was bombarded simultaneously with 6 keV X-rays from two ^{55}Fe sources, one beam being incident on the gas proportional scintillation counter side, the other being directed to the proportional counter detector. To this latter beam correspond the direct pulses. The transferred pulses, corresponding to the detection of the photons from the gas scintillation counter, have the characteristic linear rise associated with the uniform production of photons across the scintillation gap. The pulse-height ratio of the transferred and the direct pulses, taken through a charge amplifier, measures t.

Of course t is a function of HV_3-HV_2, the potential difference between grids 3 and 2 (see Fig. 3) for a given filling of the PIPS detector. As the free paths before photo-ionization in the filling of the proportional counter can be of the order of the spacing between the wires of grid 4, t is also affected by HV_3-HV_4. With grids 4 and 5 and the cathode wires of the photo-ionization detector grounded (for a fixed value of HV_3-HV_2), t increases when HV_3 decreases, becoming constant for $HV_3 \leq \leq -1$ kV. The data on transfer efficiency were obtained keeping $HV_3 = -1$ kV, and are shown in Fig. 4 for two different krypton flow rates. Both curves display the characteristic linear rise of the secondary scintillation with the applied field, in the absence of charge multiplication, and imply a threshold field for secondary light emission of $\sim$ 720 V/cm at 1 atm. The extent to which this value is affected by the impurities in the gas scintillation chamber is not known. It is quite clear that impurities are dominating the light output, the increase of this parameter being more than 50% when the flow rate is increased from 200 to 300 cm³/min.

Even so, Fig. 4 shows that a transfer ratio of about 5.5 is obtained for 3.2 kV across the scintillation gap, just before charge multiplication starts, as implied by a faster than linear rise of t with the applied voltage.

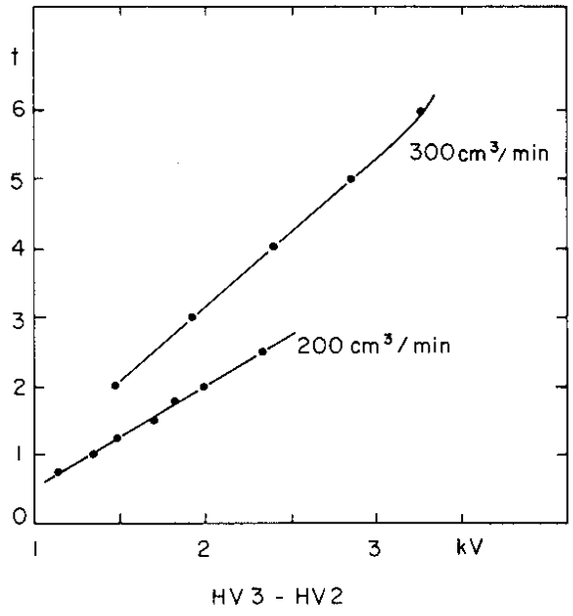

Fig. 4 Transfer efficiency versus voltage across the scintillation gap for two krypton flow rates of 200 and 300 cm³/min, respectively.

5. Energy resolution

A commercially available low-noise room temperature preamplifier was used for the energy resolution measurements and, working with the photo-ionization detector in the proportional region, the electronics noise was negligible. The resolution of this detector for the direct pulses was 15.8% for 5.9 keV, as measured with a ^{55}Fe source. Although these interactions are very well localized, compared with the wide distribution of the photoelectrons coming from the detection of photons produced in the scintillation gap, this resolution may be taken as being characteristic of the photo-ionization detector. Nevertheless, with the primary ion pair distributed like the photoelectrons corresponding to the transferred pulse, it is possible that the resolution of the photo-ionization detector for a 5.9 keV energy deposition may be better, as there is some averaging with respect to the non-uniformities of the field at the surface of the anode wires due to the discrete structure of the cathode in the proportional counter.

As no information is available either on the mean energy required for making an ion pair or on the Fano factor for the filling of the photo-ionization detector, these parameters were arbitrarily taken as 24.3 eV (the mean energy for making an ion pair in krypton, which allows the approximation $\bar{L} \simeq t$) and F = 0.17, respectively.

Figure 5 displays the expected variation of the energy resolution of the PIPS detector, corresponding to the transferred pulses, with $\bar{L}$ approximately identical to the transfer efficiency t. Two cases are considered: the average proportional counter, with a resolution of 16% for 5.9 keV (approximately the same as that obtained with direct irradiation of the photo-ionization detector); and the case of a good proportional counter with an energy resolution of 14% at the same energy, which may also reflect the better energy resolution that can be associated with the detection of the photons.

The energy resolution measurements made using the transferred pulses reflected the clear improvement that is expected when $\bar{L}$ increases, specially for small $\bar{L}$ values, the best spectrum being shown in Fig. 6 and corresponding to an energy resolution of 10.8%. It was obtained at $t \simeq 5.5$, and is in fair agreement with the data of Fig. 5.

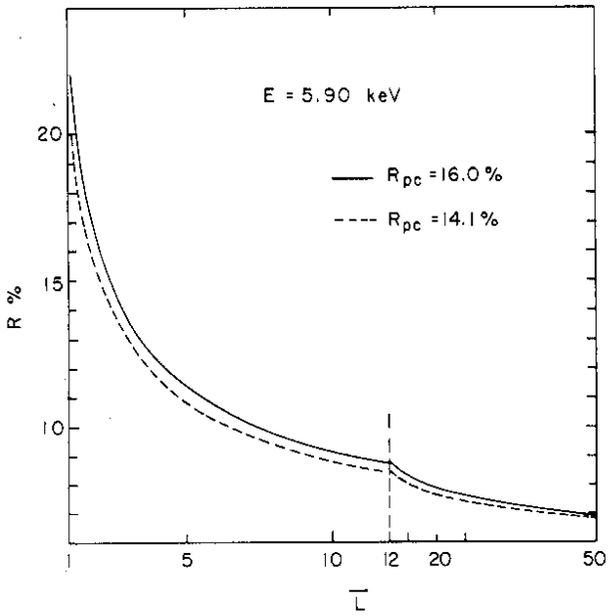

Fig. 5 Calculated energy resolution of PIPS for 5.9 keV, for photo-ionization proportional counters having 16.0% and 14.1% energy resolution as a function of $\bar{L}$, under the assumption that $\bar{L} = t$ (see text).

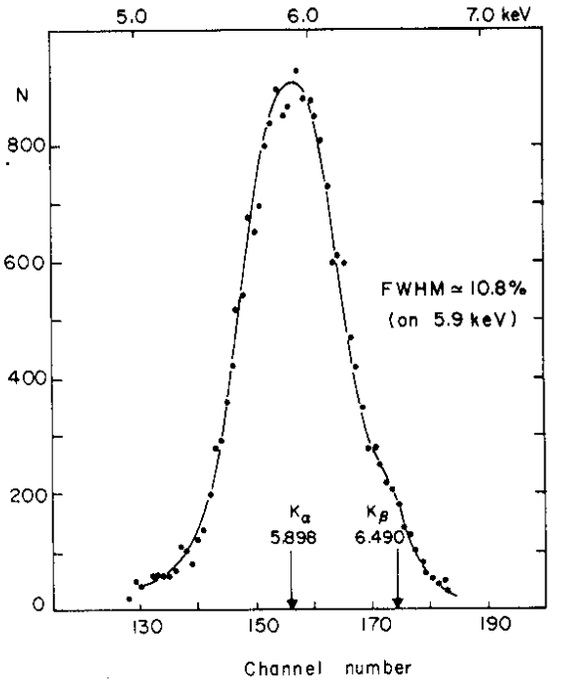

Fig. 6 Measured energy distribution of X-rays from a ^{55}Fe source. The resolution is 10.8% FWHM for the K_α line.

6. Spatial distribution

The spatial distribution of the photoelectrons on the photo-ionization detector is mainly determined by the thickness of the scintillation region, by its distance from the LiF window, and by the absorption coefficient of this window for the incident photons. The mean free path (λ) of the photons in the filling of the photo-ionization detector and the transparency of the grids will also influence this distribution.

Using anodes at 2.54 mm distance in the photo-ionization detector and taking the signal from one anode wire, this pulse height was measured as a function of the distance between the wire and a collimated beam from a ^{55}Fe source. Experimental data are shown with their error bars in Fig. 7. In the same figure, curve (a) corresponds to a calculation for the ideal case of a linear source of light in the scintillation region, and assumes that $\lambda = 0$, i.e. the photons are converted after traversing a negligible path-length in the photo-ionization detector. This is then an ideal case; however, it clearly reflects the capabilities of the PIPS detector for localization purposes. The calculation of curve (b) corresponds approximately to the experimental situation, the diameter of the light-source being about 0.8 mm, with each anode wire collecting photoelectrons over a 2.54 mm slice. The mean free path for photo-ionization was taken as 1 mm. Curve (a) is narrower than the experimental distribution, an effect that is probably due to a slight charge multiplication in the light-emitting counter because of too high voltage across the scintillation gap during the measurement.

The distribution has a FWHM of about 6.5 mm.

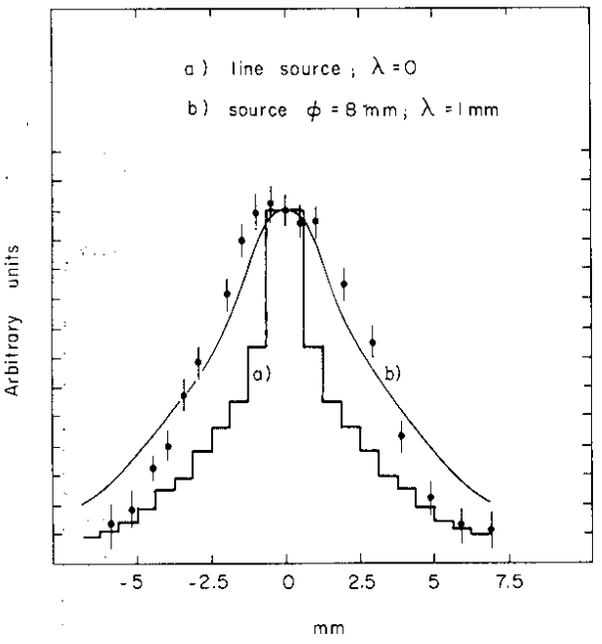

Fig. 7 The dots correspond to the experimental spatial distribution of the detected photoelectrons. The curves are computed for different values of the bin widths, of the radial dimensions of the light-source associated with the drift of electrons on the scintillation gap, and of the mean free paths for the photons on the photo-ionization detector. These last two parameters are quoted in the figure, the bin width for curve (b) being the anode wire spacing, 2.54 mm, and for curve (a) a quarter of that value.

7. Conclusions

The results that have been presented, although of a preliminary nature and obtained under conditions of purity for the gas scintillation counter that are far from the normal operating conditions for this type of detector, are of interest. They show that both energy and spatial resolutions can be obtained over large areas of detection, together with multiple hit capabilities that far exceed those of vacuum photodiodes or of photomultiplier arrays. Other important characteristics are the stability of operation associated with the absence of wavelength shifters, the possibility of working in magnetic fields, the selective blindness to external radiation, the applicability of background rejection techniques. The data obtained suggest that larger transfer ratios can be reached, implying an improvement in energy resolution, better localization, and multihit capabilities. It thus seems that PIPS takes good advantage of both the properties of gas scintillation proportional counters and multiwire proportional chambers, and that it can be useful for a wide variety of applications. It is not worth while to speculate now about using other filling gases either for the gas scintillation proportional counter or for the photo-ionization detector, as the revival of these detectors is rather recent, and information on spectral distributions of mixtures of noble gases that are good scintillators is not available.

PIPS can probably be used as a photomultiplier (or better as an image intensifier) if a conductive photosensitive layer is deposited under the window of the gas scintillation proportional counter part, the purity of the noble gas filling and the absence of charge multiplication being favourable factors.

References

1. A. Policarpo, Space Sci. Instrum. 3 (1977) 77. D.F. Anderson, Thesis, Columbia University (1978).
2. D.F. Anderson, T.T. Hamilton, W.H.M. Ku and R. Novick, Nucl. Instrum. Methods 163 (1979) 125; also, IEEE Trans. Nucl. Sci. NS-26 (1979) 490.
3. A. Peacock, R.D. Andresen, A. von Dordrecht, E.A. Leimann, G. Manzo, B.G. Taylor, R. Berthelsdorf, J.C. Culhane, J.C. Ives and R.W. Sanford, IEEE Trans. Nucl. Sci. NS-26 (1979) 486.
4. M. Mutterer, J. Pannicke, K.P. Schelhaas, J.P. Theobald and J.C. van Staden, IEEE Trans. Nucl. Sci. NS-26 (1979) 382.
5. Nguyen Ngoc Hoan, Nucl. Instrum. Methods 154 (1978) 597.
6. Nguyen Ngoc Hoan, G. Charpak and A. Policarpo, J. Nucl. Med. 20 (4) (1979) 335.
7. T. Davelaar, G. Manzo, A. Peacock, B.G. Taylor, R.D. Andresen and J.A.M. Bleeker, ESLAB/79/42 (submitted to Astronomy and Astrophysics, Sept. 79).
8. J.C. van Staden, J. Foh, M. Mutterer, J. Pannicke, K.P. Schelhaas and J.P. Theobald, Nucl. Instrum. Methods 157 (1978) 301.
9. J.E.F. Baruch, G. Broke, E.W. Kellermann, J.E. Bateman and J.F. Connolly, RL-78-004 (March 1978).
10. A. Policarpo, Nucl. Instrum. Methods 153 (1978) 389.
11. J. Seguinot and T. Ypsilantis, Nucl. Instrum. Methods 142 (1977) 377.
12. G. Charpak, S. Majewski, G. Melchart, F. Sauli and T. Ypsilantis, Nucl. Instrum. Methods 164 (1979) 419.
13. M. Suzuki and S. Kubota, Nucl. Instrum. Methods 164 (1979) 197.